INTERNATIONAL JOURNAL OF ROBOTICS
(THEORY AND APPLICATIONS)
E-mail: IJR@kntu.ac.ir

Evaluation of an Adaptive Neuro-controller for Robotic Hand Prosthesis (PARS)

M. Gohari[a,1], M. Tahmasebi[b] and Y. Abbasi[a]

[a] Faculty of Mechanical Engineering, Arak University of Technology, Arak, Iran, P.O. Box, 3818146763
[b] Markazi Agricultural and Natural Resources Research and Education Center, Agricultural Research, Education and Extension Organization (AREEO), Arak, Markazi, Iran, P.O. Box, 88938135

ARTICLE INFO

Article history:
Submit: 2025-03-06
Revise: 2025-08-04
Accept: 2025-08-09

Keywords:
Robotic Hand Prothesis
EMG Signal
Neuro Adaptive Controller
Under Actuated Hand

ABSTRACT

This paper assesses the performance of a lightweight, compact, portable, and wearable cable-driven robotic hand prosthesis called PARS (Prosthesis Adaptive Robotic System). Initially, a mathematical model was developed, followed by the design and fabrication of a Neuro controller. The functionality of the robotic hand was confirmed through both simulations and experimental tests. The pilot study demonstrated that the proposed Neuro controller effectively tracks various desired joint trajectories and performs well in real-world applications. Experimental results indicated a strong correlation between the robotic hand prosthesis (RHP) and the human hand in terms of vertical position, speed, and acceleration during flexion and extension. The Neuro controller surpassed traditional PID in stability and accuracy. This study underscores the practical potential of developing advanced tools for assisting disabled individuals. However, further improvements are needed to enhance practicality, such as integrating force sensors and making the hardware more compact. Additionally, improving the control software to support simultaneous position and active force control could boost system performance in more complex tasks.

[1] Corresponding address: Senior Researcher, PRISMA Lab, University Federico II, Naples, Italy
Tel.: 00393516159413;
E-mail address: mohammad.gohari@unina.it.

1. Introduction

Significant advancements have been achieved in the development of anthropomorphic hands over the past twenty years, leveraging new technologies for both robotic and prosthetic uses. Presently, various anthropomorphic hands are available on the market.

Drawing inspiration from the human hand, compliance and sensors have been incorporated into robotic hands using multiple technological approaches to enhance robustness by absorbing external impacts and improving object grasping and manipulation capabilities.

Elastic actuation has been implemented through methods such as series elastic tendons, compliant links made from steel layers, and elastic joints, including both flexure-based and spring-based designs [1-6].

Although the grasping abilities of robotic hands are continuously improving and nearing human performance, there remain gaps, particularly in the dexterity of in-hand manipulation, especially when dealing with deformable objects. Enhanced in-hand manipulation enhances the accuracy and efficiency of upper-limb functions, as evident in human hands.

Recently developed fully-actuated hands, such as the Shadow Dexterous Hand, the KITECH hand, and the BCL-13, have shown some level of in-hand manipulation dexterity thanks to independently driven finger joints. However, designing a fully-actuated hand is challenging, primarily due to the complexity of integrating numerous actuators.

Additionally, controlling such hands in prosthetic applications is difficult given the limited bandwidth of bio-signal interfaces available for control.

Due to these challenges, researchers are shifting their focus toward designing underactuated hands, where fewer degrees of actuation are used to control a greater number of degrees of freedom (DOFs). Recent advancements have demonstrated efficient grasping [4] and in-hand manipulation by leveraging the elasticity of underactuated fingers [7,8], thereby enhancing the functionality of these hands.

Notable examples of robotic hands with in-hand manipulation capabilities include the iRobot-Harvard-Yale (iHY) hand [5], the GR2 gripper [25], the caging manipulation gripper, and the Pisa/IIT SoftHand 2 [26].

The current paper aims to present a low-cost design of hand prosthesis that works by EMG signal, and it is controlled by an adaptive neuro controller to have superior performance.

2. Material and methods

The present robotic hand prosthesis which is called PARS includes 19 joints and is powered by three motors. The assembled robotic hand is shown in Fig. 1. In Fig.1(a), the connection of tendons to the joints are illustrated. Each finger (shown in Fig. 2) includes three flexion/extension joints made of compliant rolling joints. The thumb is equipped with one rotation joint, while the other fingers have one abduction/adduction joint, all designed as revolute joints.

The finger flexion joints use a curved shaped contact surfaces held together by elastic elements which is elastic string.

Each joint comprises a base link, a distal link, two ligaments, and a tendon. The elastic ligaments, which are attached to both the base and distal links, along with the tendon, made from the same elastic string, create the joint's multidirectional compliance.

By pulling the tendon, the distal link rolls on the curved surface of the base link, when the tendon is released, the elastic ligaments return the distal link to its extended position, akin to a torsional spring in a conventional pin joint.

This allows the joint to accommodate various disarticulations, including backward and sideways bends, twists, and dislocations.

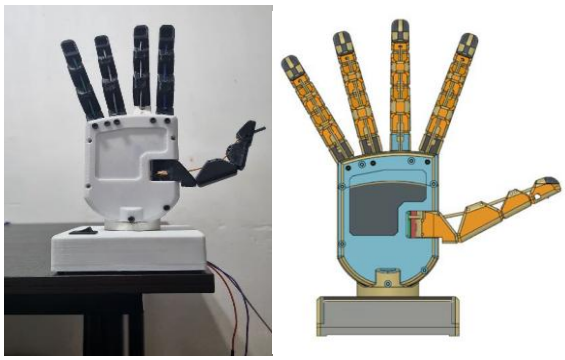

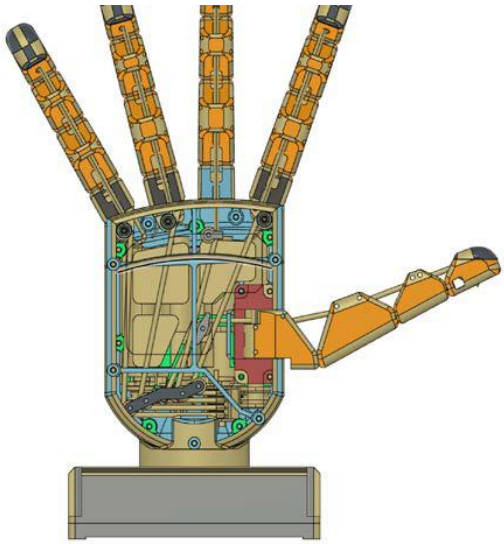

(a)

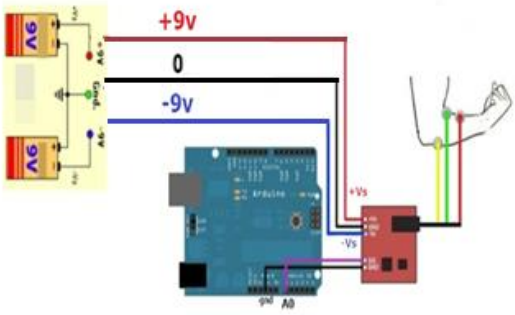

(b)

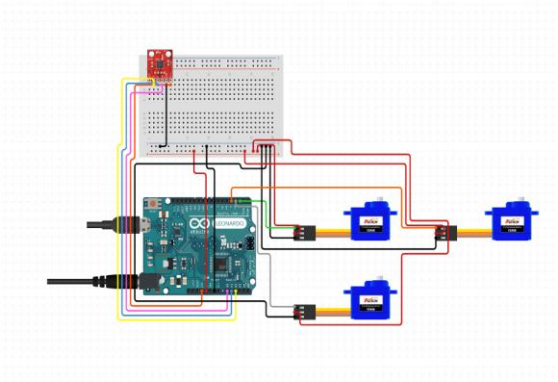

(c)

Fig. 1. (a) Robotic Hand PARS and its elements, (b) EMG signal card, (c) Servomotor's connections to the Arduino

An Arduino Uno board is used as a controller, and an EMG signal acquisition card is applied to gather muscle signals. They are unveiled in Fig. 1(b) and Fig. 1(c), respectively.

2.1. Mathematical model

To present position of the finger's tip, we need a mathematical model. Refer to Fig. 2, the coordinates of the endpoint of the fingertip is computable by the following equation:

$$x = l_1 cos\theta_1 + l_2 \cos(\theta_1 + \theta_2) + l_3 \cos(\theta_1 + \theta_2 + \theta_3) \quad (1)$$

$$y = l_1 sin\theta_1 + l_2 \sin(\theta_1 + \theta_2) + l_3 \sin(\theta_1 + \theta_2 + \theta_3) \quad (2)$$

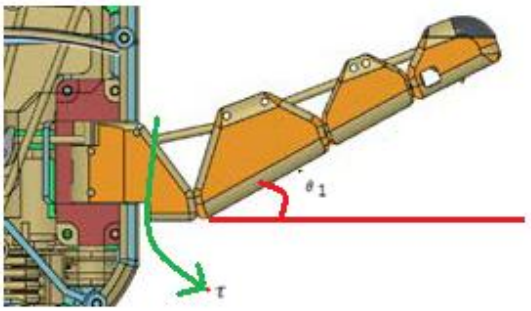

Fig. 2. Tendon driven finger (first joint active, but second and third joint are passive)

The free-body diagram of a robotic finger is shown in Fig. 2. Each link of the robotic finger phalanx can be considered as a pendulum model

which is unveiled in Fig. 3 via one degree of freedom.

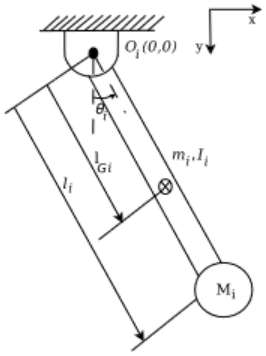

Fig. 3. Single DOF pendulum model for exoskeleton

The Lagrangian formulation is stated below to acquire a dynamic model:

$$L_i = E_{ki} - E_{pi} \quad (3)$$

$$T_i = \frac{d}{dt}\left(\frac{dL_i}{d\dot{\theta}_i}\right) - \frac{dL_i}{d\theta_i} \quad (4)$$

Where E_k and E_p represent kinematic energy and potential energy, respectively. They can be calculated as follows:

$$E_{ki} = \left(\frac{1}{2}I_i\right)\dot{\theta}_i^{\,2} + \frac{1}{2}m_i\dot{r}_{Gi}^2 + \left(\frac{1}{2}M_i\dot{r}_i^2\right).$$
$$E_{pi} = gy_{Gi}m_i + M_i gy \quad (5)$$

$$E_{ki} = \left(\tfrac{1}{2}I_i\right)\dot{\theta}_i^{\,2} + \tfrac{1}{2}m_i l_{Gi}^2\dot{\theta}_i^2 + \tfrac{1}{2}M_i l_i^2\dot{\theta}_i^2$$
$$E_{pi} = gcos\theta_i(l_{Gi}m_i + M_i l_i) \quad (6)$$

Thus, the dynamic torque can be reached as:

$$T_i = \left(m_i {l_G}^2 + M_i l_i^2 + I_i\right)\ddot{\theta}_i + b\dot{\theta}_i + (l_i M_i + l_{Gi} m_i)gsin\theta_i$$

The transfer function obtained in Laplace is as:

$$G(s) = \frac{\theta_i(s)}{T_i(s)} = \frac{1}{s^2 + \frac{b}{(m_i {l_{Gi}}^2 + M_i l_i^2 + I_i)}s + \frac{(l_i M_i + l_{Gi} m_i)g}{(m_i {l_{Gi}}^2 + M_i l_i^2 + I_i)}}. \quad (7)$$

$$\theta_i(s) = \tau(s) \times G(s) = \tau(s) \times \frac{1}{s^2 + Cs + K} \quad (8)$$

By considering torque as the tension of string "F" multiplied by the motor shaft radius of revolution "r", we have:

$$\theta_i(s) = F(s)r \times \frac{1}{s^2 + 296.95s + 261.48} \quad (9)$$

By considering bellow:
$b = 2\zeta\omega_n$ =0.0083
$\zeta = 0.5$, $\omega_n = \sqrt{mglsin\theta}$
Θ=6.61

The required values of Eq. (7) are considered from [22]**.** Thus, the relationship between phalanx angle and actuated force by tendons is obtained. The parameters are listed in table 1.

Table 1. List of parameters

PARAMETERS	VALUE
B	0.0083
ζ	0.5
C	295.95
K	261.48

2.2. Controller design and simulation

Whereas robotic hand prosthesis is exposed to many types of disturbances, an adaptive controller is required to provide robustness and stability with high accuracy [9 and 10]. To have an adaptive controller that can change its parameters regarding inputs and disturbances, a neural network is selected due to its potential for adaptability with various input signals and disturbances.
Neural network controllers are particularly beneficial in scenarios where traditional controllers may struggle [11-13], such as systems with complex, nonlinear dynamics or systems with significant uncertainties.

Artificial neural networks (ANNs) are inspired by the human brain's architecture, consisting of interconnected neurons or nodes. Each neuron processes input information and passes it to the next layer, ultimately generating an output. The basic structure of an ANN includes:

- Input Layer: The initial data input.

- Hidden Layers: Intermediate layers that perform calculations.
- Output Layer: The final output.

The ANN learns by adjusting the weights of the connections between neurons using training algorithms, typically through backpropagation, to minimize the error between the predicted and actual output [14].
Each neuron j receives input signals x_i and generates an output y_i. The input to the neuron is a weighted sum of the inputs plus a bias b_j.

$$u_j = \sum x_i w_{ji} + b_j \quad (10)$$

The neuron applies an activation function ϕ to this input to produce the output:

$$y_j = \varphi(u_j) \quad (11)$$

Common activation functions include the sigmoid function, hyperbolic tangent (tanh), and ReLU (Rectified Linear Unit). In this controller, the hyperbolic tangent is used:

$$\varphi(u) = \tanh(u) \quad (12)$$

A feedforward neural network with one hidden layer can be represented as:

$$y_k = \varphi(\sum \sum_j w_{jk}\, \varphi\big(\sum x_i w_{ji} + b_j\big) + b_k) \quad (13)$$

Here:
w_{ji} and w_{kj} are weights for the input-to-hidden and hidden-to-output layers, respectively.
b_j and b_k are biases for the hidden and output layers, respectively.

2.2.1. Neural network controller

In the context of control systems, a neural network controller aims to determine the control input *u(t)* to drive a system's state *x(t)* to a desired state $x_d(t)$ The neural network can approximate the control law *u(t)* based on the system's state and possibly its derivatives.

2.2.2. Control law

The control input *u(t)* is generated by the neural network as follows [15 and 16]:

$$u(t) = \varphi(W_2 \varphi(W_1 x(t) + b_1) + b_2) \quad (14)$$

Where
X(t) is the state vector of the system.
W_1 and W_2 are the weight matrices for the input-to-hidden and hidden-to-output layers, respectively.
b_1 and b_2 are the bias vectors for the hidden and output layers, respectively. ϕ is the activation function.

2.2.3. Training the neural network

The neural network controller is trained using a dataset of input-output pairs. The training involves adjusting the weights and biases to minimize a cost function J, typically the mean squared error (MSE) between the desired output u_d and the network output *u*:

$$J = \frac{1}{N}\sum_{i=1}^{N}(u_d(i) - u(i))^2 \quad (15)$$

The backpropagation algorithm is commonly used for training, which involves calculating the gradient of J with respect to the weights and biases and updating them iteratively:

$$w_{ji} \leftarrow w_{ji} - \eta \frac{\partial J}{\partial w_{ji}} \quad (16)$$

$$b_j \leftarrow b_j - \eta \frac{\partial J}{\partial b_j} \quad (17)$$

where η is the learning rate. The training step should be done by proper samples in number and validity [17].
Regards to stated benefits of the neuro controller, the neural network with feed-forward back propagation configuration is trained by an error signal and control signal which is derived from the PID controller. It includes 6 hidden layers and 10 neurons in each layer (Fig. 4). After the training process, it is used in Simulink Software for evaluations (Fig. 5). The input of neuro controller is error signal which is error between output position and desired position.
The PD controller coefficients which are used in training are K_p=50000 and K_d=500. The primary coefficients of PD controller are reached by Ziegler- Nichols method, then neuro controller is trained by that via offline technique.

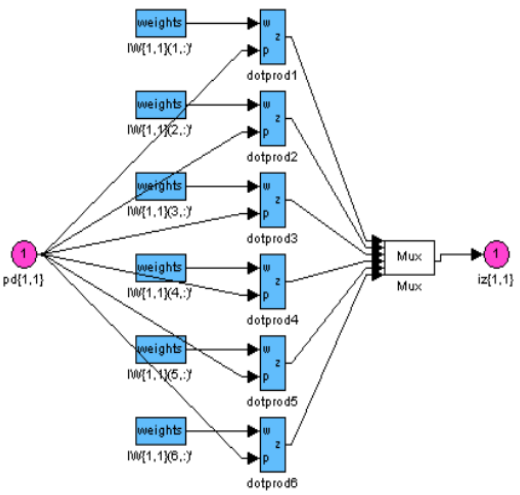

Fig. 4. Architecture of ANN

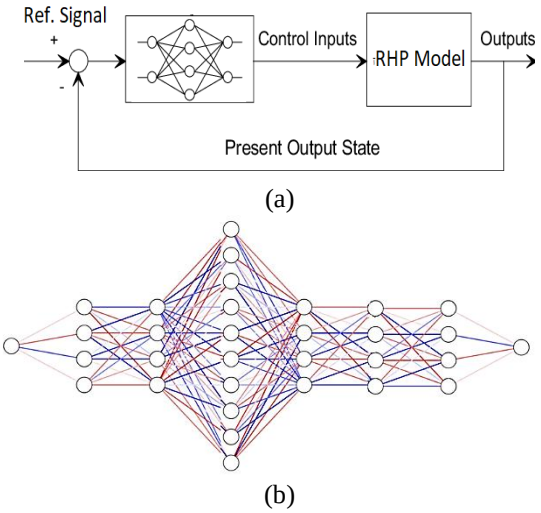

(a)

(b)

Fig. 5. The ANN used as a controller for the Hand exoskeleton (a), the structure of used NN (b)

Results show that the Neuro controller is stable when input is sawtooth signal (Fig. 6) or Sine signal (Fig. 8). In Fig. 7, it can be seen its accuracy to reach the desired value is higher than PID.

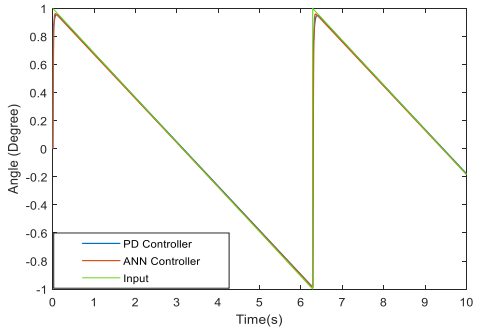

Fig. 6. Comparison between PID and ANN controllers (green line is ANN controller and blue is PID controller**)**

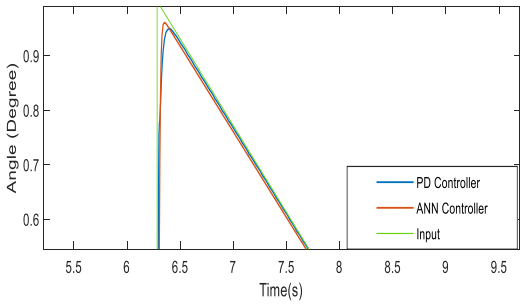

Fig. 7. Zoom of saw tooth signal with comparison between PID and ANN controllers (red line is ANN controller and blue is PID controller)

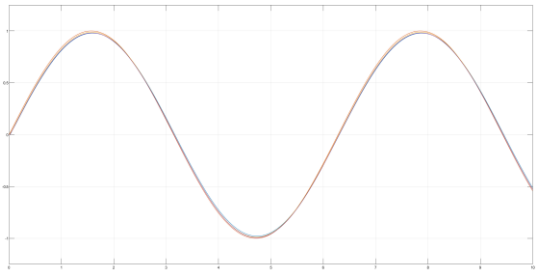

Fig. 8. Responses of the system by Sine wave

Moreover, Fig. 9 illustrates that the performance of the ANN controller is higher than PID when the system is exposed to the square signal. Fig. 10 shows it by zoom.

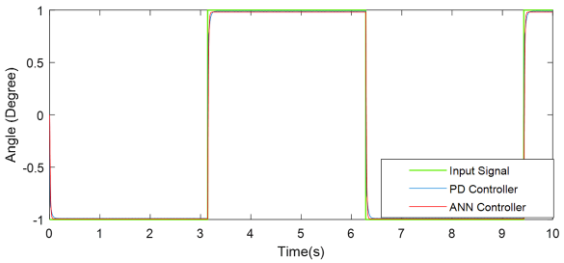

Fig. 9. Output of the system by square signal**.**

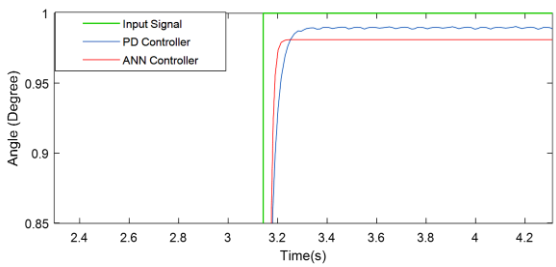

Fig. 10. Output of the system by square signal by zoom.

Thus, this Neuro controller which is evaluated by simulation assessment is implemented on the experimental testbed.

3. Results and discussion

The fabricated robotic hand prosthesis and EMG signal recorder are connected to the Arduino board same as other efforts [18-20]. The hardware components—including sensors, microcontrollers, and actuators—were carefully selected based on three key criteria: **cost**-effectiveness, energy efficiency, and ease of implementation. This section outlines the systematic integration process, covering:

1. Signal Acquisition: High-sensitivity EMG sensors capture muscle activity with minimal noise.
2. Data Processing: Microcontrollers (Arduino Nano) filter and amplify signals in real time.
3. Actuation Control: Precision motors translate processed signals into mechanical outputs.

The workflow ensures low-latency conversion (<50 ms) of neuromuscular signals to functional movements, validated through bench testing. These parts were selected based on their reliability, availibility, and suitability for the proposed application, forming the foundation of an effective and responsive system.

- Arduino Uno: main controller for processing EMG signals and leading motor actuation.
- BITalino (r)evolution Board: Captures muscle activity by three electrodes
- Servo Motor SG90: Controls finger actuations
- External 12 V Power Supply: Powers the system and motors.
- Programmer USB-serial: Facilitates Arduino programming.

The EMG signal is processed by a code in the Arduino card. The RHP is tested by a camera recorder. The recorded movie is post-processed by Kinovea Software. A pixel is marked on the human fingertip and another one is marked on an RHP fingertip. It is demonstrated in Fig. 11.
The position, speed, and velocity of RHP fingertip and human fingertip are measured during flexion and extension. As can be seen in Fig. 12, there is good convergence between RHP and human fingertip in vertical position.
Also, a little bit of delay can be observed in this movement. It shows the selected mathematical model [21] is properly fitted.

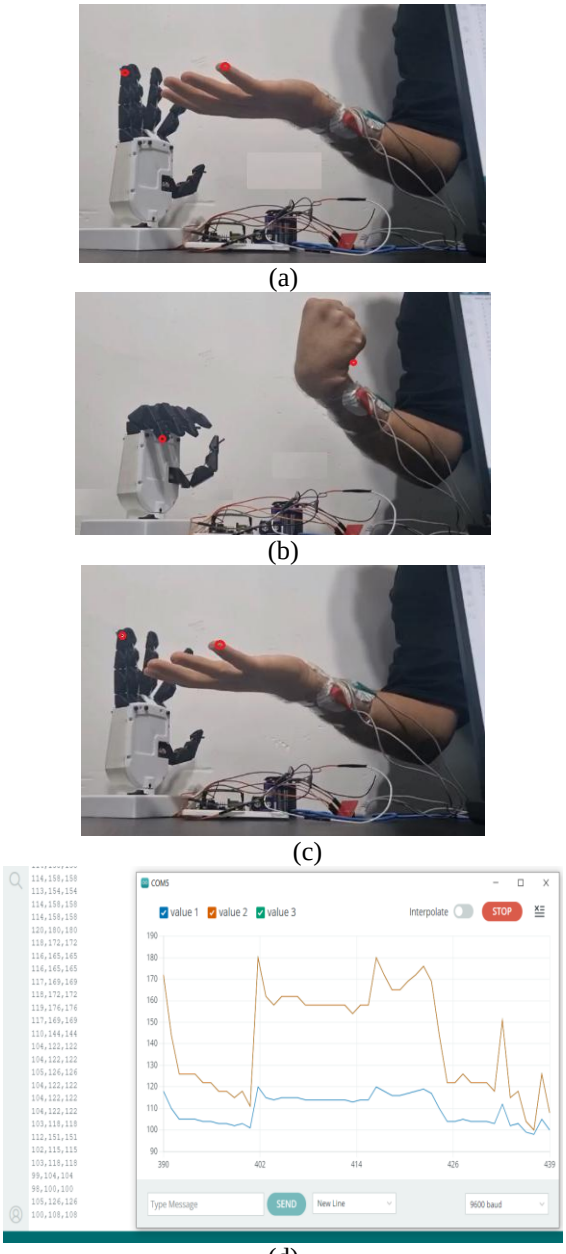

Fig. 11. Tracking of flexion and extension of PARS controlled by EMG signal at marked pixel; (a) extension, (b) flexion, (c) extension, and (d) EMG Signals in three electrodes installed on the wrist

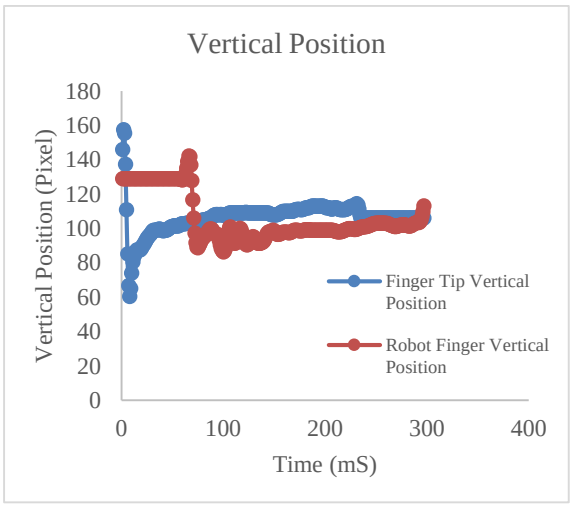

Fig. 12. Vertical position in RHP fingertip and human fingertip

Furthermore, the total displacement of both marked pixels is measured by software and is unveiled in Fig. 13. The closeness between values is high, and the trend of motion is in common. Additionally, the speed and acceleration of the marked point (pixel) are measured at the human fingertip and RHP fingertip and exploited in Fig. 14 and 15, respectively.

As can be observed, the speed of RHP movement is very close to the human fingertip. This issue is reported in the other studies also [22-24].

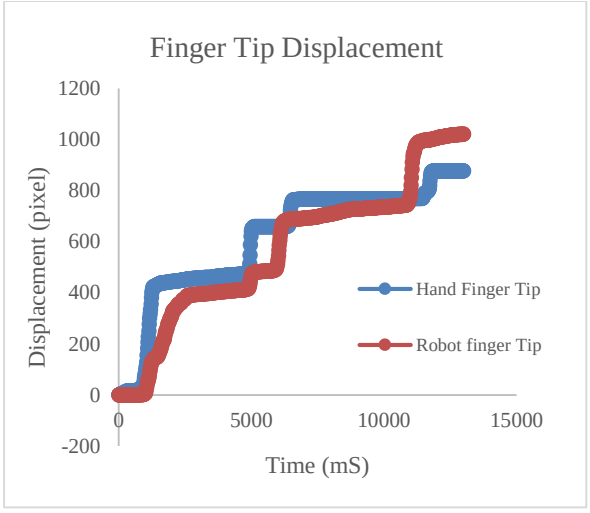

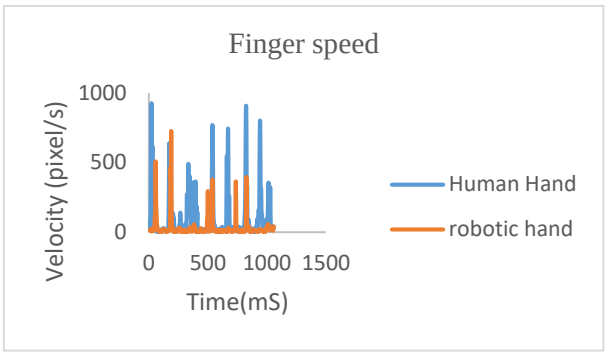

(b)

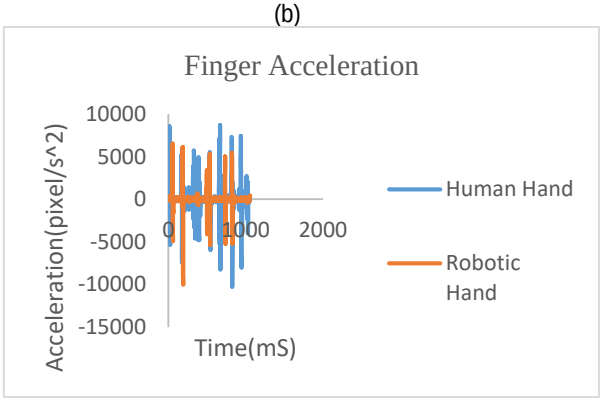

(c)

Fig. 13. Displacement in RHP fingertip and human fingertip (a), speed (b), and acceleration of fingertip at marked point (c)

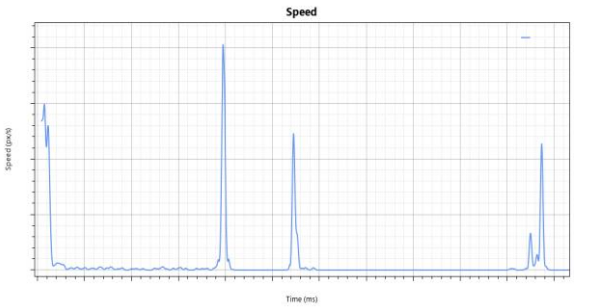

(a)

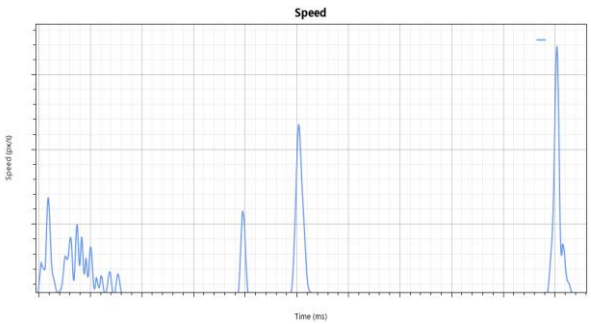

(b)

Fig. 14. Speed of fingertip at marked point: (a) human, (b) RHP

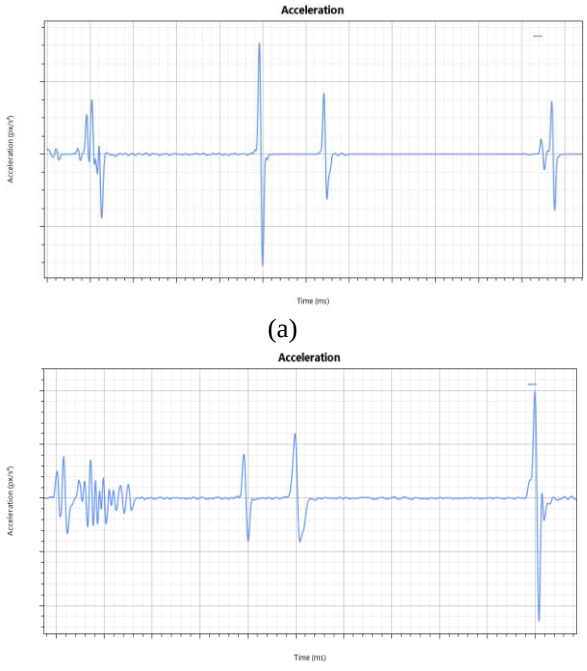

Fig. 15. Acceleration of fingertip at marked point: (a) human, (b) RHP

The results of experimental tests show that the response times of prosthesis is reasonable while in other assessment this kind of video measurements for evaluations were not used [22-24]. In fact, they focused to force sensor measurement of fingers and kinematic responses are ignored [18 and 19], but current research is studying accuracy in terms of motion parameters.

4. Conclusions

In this study, the effectiveness of a lightweight, simple, portable, and wearable cable-driven hand robot was assessed. Initially, a mathematical model was considered for PARS, and Neuro controller was analyzed, and fabricated. The PARS functionality was then verified using a simulation.

The pilot simulation study demonstrated that the suggested Neuro controller performance is suitable for this application, capable of tracking various desired joint trajectories.

Moreover, the experimental assessment shows that the response time and trajectory of PARS are common to the human hand. Besides, the speed and acceleration of PARS are fast as much as the human hand in flexion and extension of the finger. This research aimed to prove the practicality of developing real tools for assistance for disabled persons.

However, further modifications are needed to enhance practicality. One crucial aspect is ensuring creating a force sensor for that. Nevertheless, a more advanced design could potentially make all the hardware more compact. Additionally, the system's control software could be improved to offer more functionality. While the Neuro control strategy presented here might be effective for practical applications, developing simultaneous position and active force control methods could enhance the system's performance in more complex tasks.

References

[1]. M. Grebenstein, M. Chalon, W. Friedl, S. Haddadin, T. Wimb¨ock, G. Hirzinger, and R. Siegwart, “The hand of the dlr hand arm sys- tem: Designed for interaction,” The Int. J. Robotics Res., Vol. 31, No. 13, pp. 1531–1555, (2012).

[2]. K. Y. Choi, A. Akhtar, and T. Bretl. "A compliant four-bar linkage mechanism that makes the fingers of a prosthetic hand more impact resistant." In 2017 IEEE Int. conf. on robotics and automation (ICRA), pp. 6694-6699. IEEE, (2017).

[3]. J. T. Belter and A. M. Dollar. "Novel differential mechanism enabling two DOF from a single actuator: Application to a prosthetic hand." In 2013 IEEE 13th Int. Conf. on Rehabilitation Robotics (ICORR), pp. 1-6. IEEE, (2013).

[4]. A. M. Dollar and R. D. Howe, “The highly adaptive sdm hand: Design and performance evaluation,” The Int. J. of Robotics Res., Vol. 29, No. 5, pp. 585–597, (2010).

[5]. L. U. Odhner, L. P. Jentoft, M. R. Claffee, N. Corson, Y. Tenzer, R. R. Ma, M. Buehler, R. Kohout, R. D. Howe, and A. M. Dollar, “A com- pliant, underactuated hand for robust manipulation,” The Int. J. of Robotics Res., Vol. 33, No. 5, pp. 736–752, (2014).

[6]. F. Lotti, P. Tiezzi, G. Vassura, L. Biagiotti, G. Palli, and C. Melchiorri. "Development of UB hand 3: Early results." In Proc. of the 2005 IEEE int. conf. on robotics and automation, pp. 4488-4493. IEEE, (2005).

[7]. M. G. Catalano, G. Grioli, E. Farnioli, A. Serio, C. Piazza, and A. Bicchi, “Adaptive synergies for the design and control of the pisa/iit softhand,” The Inte. J. Robotics Res., Vol. 33, No. 5, pp. 768–782, (2014).

[8]. C. Rossi, S. Savino, V. Niola, and S. Troncone. "A study of a robotic hand with tendon driven fingers." Robotica 33, No. 5, pp.1034-1048. (2015).

[9]. M. Yin, D. Shang, T. Xu, and X. Wu. "Joint modeling and closed-loop control of a robotic hand driven by the

tendon-sheath." IEEE Robotics and Automation Letters 6, No. 4, PP. 7333-7340, (2021).
[10]. F. Cursi, V. Modugno, and P. Kormushev. "Model predictive control for a tendon-driven surgical robot with safety constraints in kinematics and dynamics." In 2020 IEEE/RSJ Inter. Conf. on Intelligent Robots and Systems (IROS), pp. 7653-7660. IEEE, (2020).
[11]. U. Safeer, Q. Khan, and A. Mehmood. "Neuro-adaptive fixed-time non-singular fast terminal sliding mode control design for a class of under-actuated nonlinear systems." Int. J. of Control 96, No. 6, pp.1529-1542, (2023).
[12]. O. Elhaki, K. Shojaei, A. Mohammadzadeh, and S. Rathinasamy. "Robust amplitude-limited interval type-3 neuro-fuzzy controller for robot manipulators with prescribed performance by output feedback." Neural Comp. and App. 35, No. 12, pp. 9115-9130, (2023).
[13]. M. Mohaghegh, S. Saeedinia, and Z. Roozbehi. "Optimal predictive neuro-navigator design for mobile robot navigation with moving obstacles." Frontiers in Robotics and AI 10 pp.1226028, (2023).
[14]. R.T. Tachiquingutierrez, A. Lay-Ekuakille, C. Chiffi, S.P. Singh, K.S. Rao."Design, fabrication, and testing of a microelectronic controller for sensing and actuating in robotic neurorehabilitation." IEEE Sensors J. 23, No. 16, pp.18700-18707, (2023).
[15]. D.K. Mishra, A. Thomas, J. Kuruvilla, P. Kalyanasundaram, K.R. Prasad, A. Haldorai. "Design of mobile robot navigation controller using neuro-fuzzy logic system." Comp. and Elect. Eng. No.101, pp.108044, (2022).
[16]. M. Tahmasebi, M. Gohari. "Design and Simulation of an Adaptive Neuro-Controller for a Wire-Driven Flexible Arm Robot." (2023).
[17]. M. Gohari, R. A. Rahman, R. I. Raja, and M. Tahmasebi. "New biodynamical model of human body responses to vibration based on artificial neural network." In 14th Asia Pacific Vib. Conf., Dyn. for Sust. Eng. Hong Kong SAR, China: Hong Kong Polytechnic University, (2011).
[18]. F. Ficuciello, G. Pisani, S. Marcellini, and B. Siciliano. "The PRISMA Hand I: A novel underactuated design and EMG/voice-based multimodal control." Eng. Appl. of Art. Intelligence 93, pp.103698, (2020).
[19]. D.E. Canbay, P. Ferrentino, H. Liu, R. Moccia, S. Pirozzi, B. Siciliano, F. Ficuciello. "Calibration of tactile/force sensors for grasping with the PRISMA Hand II." In 2021 IEEE/ASME Int. Conf. on Adv. Inte. Mechatronics (AIM), pp. 442-447. IEEE, (2021).
[20]. H. Liu, P. Ferrentino, S. Pirozzi, B. Siciliano, F. Ficuciello. "The PRISMA Hand II: a sensorized robust hand for adaptive grasp and in-hand manipulation." In The Int. Symp. of Robotics Res., pp. 971-986. Cham: Springer International Publishing, (2019).
[21]. M. Soleimani Amiri, R. Ramli, M.F. Ibrahim, D. A. Wahab, and N. Aliman. "Adaptive particle swarm optimization of pid gain tuning for lower-limb human exoskeleton in virtual environment." Math. 8, No. 11, pp.2040, (2020).
[22]. P. Chivapornthip, E.L.J. Bohez, S. Nanthavanij, K. Sitthiseripratip, and E. Lorprayoon. "Biomechanics of index finger during mouse click." In The Third Int. Conf. on the Dev. of Biomedical Engi. in Vietnam: BME2010, 11–14 January, 2010, Ho Chi Minh City, Vietnam, pp. 51-54. Springer Berlin Heidelberg, (2010)
[23]. F. Ficuciello, "Hand-arm autonomous grasping: Synergistic motions to enhance the learning process." Intel. Ser. Robotics 12, No. 1, pp.17-25, (2019).
[24]. F. Ficuciello. "Synergy-based control of underactuated anthropomorphic hands." IEEE Trans. on Ind. Informatics 15, No. 2, pp.1144-1152, (2018).
[25] Rojas, N., Ma, R. R., & Dollar, A. M. (2016). The GR2 gripper: An underactuated hand for open-loop in-hand planar manipulation. IEEE Transactions on Robotics, 32(3), 763-770.
[26] Della Santina, C., Piazza, C., Grioli, G., Catalano, M. G., & Bicchi, A. (2018). Toward dexterous manipulation with augmented adaptive synergies: The pisa/iit softhand2. IEEE Transactions on Robotics, 34(5), 1141-1156.

Biography

Mohammad Gohari holds a PhD in Mechanical Engineering from UTM University, Malaysia. He completed his first postdoctoral fellowship in the field of artificial intelligence in rotor fault detection using vibration signals at UTM. He has been a faculty member of Arak University of Technology since 2013 and is working in the field of vibration control. He is currently working as a Senior Researcher at PRISMA LAB Robotics Laboratory, Federico II University, Italy, in the field of robotics application in medical engineering. One of his research topics is the application of robotics in Rehabilitation and Surgical Robots with a vibration control approach.

Mona Tahmasebi recieved her PhD in Mechanical Engineering from UTM University, Malaysia. Currently she is assistant professor at Agricultural and Natural Resources Research and Education Center, Agricultural Research, Education and Extension Organization (AREEO), Arak. She is working in Smart farming and robotics.